CONDUCTIVITY AND CARDIOMYOCYTE COMPATIBILTY OF POLY LACTIC-CO-GLYCOLIC ACID CARBON NANOFIBER COMPOSITES

D.A. Stout[1], J. Yoo[2], T.J. Webster[1,3,*]
[1] School of Engineering, Brown University, Providence, Rhode Island, 02917 USA, [2] Division of Biology and Medicine, Brown University, Providence, Rhode Island, 02917 USA, [3]Department of Orthopedics, Brown University, Providence, Rhode Island, 02917 USA
* Corresponding author (Thomas_Webster@Brown.edu)

Keywords: *Carbon Nanofiber, Poly Lactic-Co-Glycolic Acid, Cardiomyocyte, Cytocompatibility*

1 Introduction

Cardiomyocytes (a specialized contractile muscle cell that generates part of the myocardium tissue of the heart) and neurons (an electrically excitable cell that processes and transmits certain information by electrical and chemical signaling in the heart [1,2]) depends on continuous conductivity to function [3]. However, such conductivity may break down during heart disease or malfunction. For instance, a myocardial infarction, also known as a heart attack, usually occurs because a major blood vessel supplying the heart's left ventricle is suddenly blocked by an obstruction, such as a blood clot [4]. During myocardial infarction, part of the cardiac muscle, or myocardium, is deprived of blood and therefore oxygen, which destroys cardiomyocytes and neurons leaving dead tissue [5] as well as denervation of the myocardium [6]. In particular, nerve damage to cardiac tissue can result in nerve sprouting in the left ventricle [6] and development of arrhythmias [7]. Scarred cardiac muscle results in heart failure for millions of heart attack survivors worldwide. In 2009, an estimated 785,000 Americans had a new coronary attack and about 470,000 had a recurrent heart attack leading to a coronary event [8].

In recent years, various techniques have been developed to promote cardiomyocyte and neuron growth around dead tissue after a myocardial infarction. Each approach has their own advantages [9], as well as disadvantages [9], but in general, all of the above can be divided into two groups: a) conductive cardiovascular patches (using scaffolding and 3D printing techniques usually with polypyrrole) and b) non-conductive cardiovascular patches (mostly involving direct cell injection, scaffolding, and injectable scaffolds). One can also observe that cardiovascular biomaterials can be either based on biodegradable or on non-biodegradable materials. Within this matrix of conductive vs. non-conductive and biodegradable vs. non-biodegradable material lie the most commonly studied materials and techniques used for promoting heart health. However, one area that has been largely omitted to date is the exploration of nanotechnology (or materials with one dimension less than 200nm) in cardiovascular applications. Numerous articles suggest that using nanotechnology can specifically promote cell functions on a variety of materials, ranging from titanium to silicon [10] due to optimal surface chemistry and wettability which control protein adsorption onto the surface. While some degree of nanostructured features may promote tissue growth, it is also known that certain topographies can hinder cell activity [11]. For example, when comparing nano to micro diamond features, Yang et al. showed that osteoblast (or bone forming cell) adhesion and proliferation increased on the nano-rough topography [11]. On the contrary, using a 1718 gene microarray, Dalby et al. were able to suggest that nano-rough topographies greater than 40 nm decreased human fibroblast cell adhesion [12].

For the above reasons, the purpose of this present study was to fabricate and evaluate cardiomyocyte and neuron functions on a novel conductive-biodegradable composites. A model polymer was used consisting of poly lactic-co-glycolic acid (PLGA) since it has been approved by the Food and Drug Administration (FDA) for therapeutic devices and has desirable biodegradable and biocompatible properties [13]. More importantly, carbon nanofibers (CNFs), which are conductive and are usually grown by catalytic decomposition of certain hydrocarbons [14], can transform non-conductive polymers to be conductive and can be made to mimic natural proteins like collagen [15]. Thus, the aim of this study was to determine if the

cytocompatibility properties of PLGA could be improved through the addition of CNFs.

2 Experiments

2.1 Fabrication

Purified carbon nanofibers (CNFs) (99.9% by weight %, Catalytic Materials, MA) with diameters of 60, 100, and 200 nanometers were sonicated in 20 ml of chloroform at 20W for 30 minutes. Two pellets of poly-lactic-co-glycolic acid or PLGA (50:50 PLA:PGA wt.) (Polysciences Cat #23986) were diluted in a 50 ml flask with 30 ml of tetrahydrofuran and were sonicated in a water bath below 30 ^{0}C for thirty minutes.

After the PLGA and CNF solutions were prepared, various PLGA:CNF weight percent ratios were created (100:0, 75:25, 50:50, 25:75, 0:100) by adding the appropriate amount of CNF to PLGA in 20 ml disposable scintillation vials. When the appropriate ratios were reached, each composite material was sonicated at 10W for 20 minutes. 1 ml of the appropriate PLGA:CNF solution was placed onto a glass substrate and then placed into an oven below 50 ^{0}C for 15 minutes. Each composite film was then vacuum dried at -20 inches of Hg gauge pressure for 48 hours to allow the THF and chloroform to evaporate.

2.2 Composite Characteristics

A Hitachi 2700 scanning electron microscope was used to characterize the surface of the PLGA:CNF samples. The electrical resistance of the PLGA:CNF samples was determined using a multi-meter (HP 34401A) by connecting two probes, via alligator clip connectors, of the meter to opposite ends of the sample. The sample was tested dry at room temperature and at opposite ends of the sample, which were 22mm apart. Three measurements were taken for each sample.

X-Ray diffraction (Bunker AXS: D8 Focus) was used with settings at 0.5° per 2 minutes between 2□ = 10-35° to characterize the crystallinity of the composites. Also, Raman spectroscopy results were obtained and recorded using an argon ion laser attached with a spectrophotometer (Acton Research Corporation, model AM505F). A low laser power of 7mW was applied to avoid any local surface heating. To acquire the spectrum, an incident light with a wavelength of 514.5 nm was used in a wavenumber region of 200–3700 cm^{-1}. The scattered radiation was collected at 180° (backscattered geometry) to the incoming beam and detected using a CCD cooled to -120°C. The spectral resolution of the Raman experimental set up was better than 1 cm^{-1} and the total integration time was 3 minutes.

2.3 Cytocompatibility

All samples and controls were sterilized using ultraviolet light for 24 hours prior to cell seeding. Human cardiomyocytes (Celprogen, Cat #36044-15) were seeded in human cardiomyocyte complete stem cell culture growth media with serum (Celprogen, Cat #M36044-15S) at a cell concentration of 3.5 x 10^4 cells/cm^2 for the cell adhesion assay and 1.5 x 10^4 cell/cm^2 for the cell proliferation assay. Cells were seeded into 12-well human cardiomyocyte stem cell culture extra-cellular matrix plates (Celprogen, Cat #E36044-15-12Well) on PLGA:CNF samples, and 22 mm diameter microscope cover slips as controls. Samples were incubated for 4 hours for the cell adhesion assay and 1, 3, and 5 days for the proliferation assay under standard incubation conditions (at 5% CO_2 95% humidified air and 37^{0}C, changing the media every other day). Two protocols were used and compared to determine cell attachment and proliferation, flourescence microscopy with DAPI staining and an MTS assay.

Troponin-I ELISA biomarker assays were completed in conjunction with the proliferation assay. This was done to make sure that the cardiomyocytes had the appropriate protein complexes that are specific to cardiomyocyte cell characteristics and did not differentiate throughout the experiment or loose phenotypes.

2.4 Statistical Analysis

All proliferation assays were performed at least in triplicate and results were compared to a controlled glass surface at 1, 3, and 5 days. Short-term adhesion assays were also performed in triplicate and compared to controlled glass surface after 4 hours of seeding. Counting of cardiomyocytes was determined for at least 5 randomly chosen microscope fields (magnification at x10) for each sample. Data were plotted as mean ± standard error of the mean and statistical analyses were performed. When data were compared, ANOVA software and a

student T-test were used. A p-value of < 0.05 was considered to be significant.

3 Results

3.1 Material Properties

Scanning electron microscopy showed that the CNFs were uniformly dispersed within the PLGA material and more CNFs were observed at higher CNF ratio samples. It was shown that increasing the CNF weight ratio in PLGA increased conductivity of the sample. Comparing the same sample weight ratio with different CNF sizes, it was shown that decreasing the CNF size increased sample conductivity (Fig. 1). Also, XRD spectra obtained from the as-synthesized PLGA:CNF composites are shown in Fig. 2. As expected an extremely broad and flat peak was recorded for the PLGA matrix, confirming its amorphous nature. However, with the addition of CNF in PLGA, the characteristic X-ray peak at $2\theta = 26.5°$ evolved into a rather strong and sharp peak in PLGA:CNF composites for the 25:75 [PLGA:CNF (wt:wt)] ratio. The curves were fitted to the characteristic peak by Gaussian distribution. Clearly, the intensity increased as full width at half maximum (FWHM) decreased as CNFs were added.
Complimentary evidence of the confirmation of the crystallinity was obtained using Raman spectroscopy and the results are provided in Fig. 3. Two sets of Raman bands are clearly visible in the composites with one set of a Raman shift at 173 and 278 cm^{-1} recorded in the presence of CNF. These Raman bands are characteristic of C-C bonds [29]. The Raman bands at 1345 cm^{-1} and 1570 cm^{-1} arose particularly due to C=C bending or bonding [29]. Another observation was the slight shift of these Raman bands in higher CNF containing PLGA composites or with 100% CNF.

3.2 Cytocompatibility

Results indicated that PLGA:CNF composites promoted human cardiomyocyte adhesion and proliferation. General trends were seen between each CNF size (Fig. 4). For 200nm CNFs, it was determined that the 25:75 ratio [PLGA:CNF; (wt:wt)] had the highest cardiomyocyte density whereas the lowest density was on the 100:0 ratio [PLGA:CNF; (wt:wt)] for both adhesion and proliferation assays. For 100nm CNFs, it was determined that the 75:25 ratio [PLGA:CNF; (wt:wt)] had the highest cardiomyocyte density whereas the lowest density was on the 100:0 ratio [PLGA:CNF; (wt:wt)] for both the adhesion and proliferation assay. For 60nm CNFs, it was determined that the 75:25 ratio [PLGA:CNF; (wt:wt)] had the highest cardiomyocyte density whereas the lowest density was on the 100:0 ratio [PLGA:CNF; (wt:wt)] for both the adhesion and proliferation assay.
Troponin-I assays indicated that cardiomyocytes had a functional Troponin Complex throughout the cytocompatible assays. For both 60nm, 100nm and 200nm CNF diameter experiments each day showed a slight increase of Troponin-I indicating more cell proliferation and production. It is also good to note that both Troponin-I assays for both 200nm and 100nm (Fig. 5) CNF diameter experiments presented the same trends seen in the proliferation cytocompatibility assays.

4 Discussion

Many materials have been developed to promote cardiomyocyte and neuron function. Recently, it has been shown that composite materials composed of different matrices (conductive vs. non-conductive and biodegradable vs. non-biodegradable) can stabilize heart tissue to decrease the consequences of a myocardial infarction and such approaches include but are not limited to: culturing patient tissue [16], direct cell injection [17], biomaterial scaffolds (materials ranging from elastin to 3D PLGA fibers) [18], 3D printing [19], and injectable scaffolds using fibrin based materials [20]. This present work assessed a brand new material, PLGA:CNF composites, for enhancing conductivity and cytocompatibility properties necessary for cardiovascular applications.
Results showed improved cardiomyocyte and neuron functions on composites with greater CNF in PLGA. It is worth speculating why greater cardiomyocyte densities were observed on such composites with increasing CNF in PLGA. Researchers found that the adsorption and bioactivity of vitronectin increases on nanophase ceramics and that this enhanced osteoblast functions (from adhesion, proliferation, and differentiation) [21]; these studies reported the closer the nanometer roughness of bone

was emulated in ceramics, the more bone growth that resulted on nanophase ceramics [21].

Clearly, CNFs possess nanoscale geometries which imitate the extracellular matrix of various tissues (such as the heart), potentially leading to improved cytocompatibility properties of these materials [22]. Although requiring further study, nanotechnology (or the use of CNFs) can play a similar important role towards promoting cardiomyocyte and neuron density by increasing vitronectin and laminin adsorption, which in turn will induce cell adhesion and proliferation. While the mechanism of enhanced cardiomyocyte and neuron density is not thoroughly known at this time, it could have to do with the topography of PLGA:CNF composites which control protein adsorption events. Importantly, it is also known that a material can be too rough and can hinder cellular activity [11]. Yang et al. used diamond films with nanometer and micron scale topographies, fabricated through microwave plasma enhanced chemical-vapor-deposition and hydrogen plasma treatment and showed that micro-sized diamond topographies decreased osteoblast cell adhesion and proliferation compared to nano-sized diamond topographies [11].

In addition, the present results showed that when adding CNFs to PLGA, the composite became conductive, whereas the PLGA matrix alone was not conductive. Pedrotty et al. showed that numerous cardiac cell functions (including adhesion, proliferation, and migration) may be modulated by electrical stimulation [23], hence requiring the use of a conductive material in cardiac applications. Also, Mihardjo et al. demonstrated that enhanced myocardial repair following an ischemic injury could be achieved using conductive polymers, such as polypyrrole [24]. The conductivity values measured in the present work were lower than that of the heart tissue (ranging from 0.16 S/m longitudinally to 0.005 S/m transversely) [25], but future techniques (such as CNF alignment) may increase the anisotropic conductivity [26] to match that of heart tissue.

5 Conclusions

In this study, it was shown that adding CNFs to PLGA improved the conductivity and compatibility properties of PLGA for myocardial tissue engineering applications. Different PLGA:CNF ratios were created to improve conductivity and cytocompatibility properties with human cardiomyocytes. It was further shown that increasing CNF weight ratio and decreasing CNF size, increased composite conductivity. In this manner, the results of this study suggest that CNFs should be further studied in cardiac tissue engineering applications**.**

6 Acknowledgements

The authors thank the Hermann Foundation for funding.

7 Figures

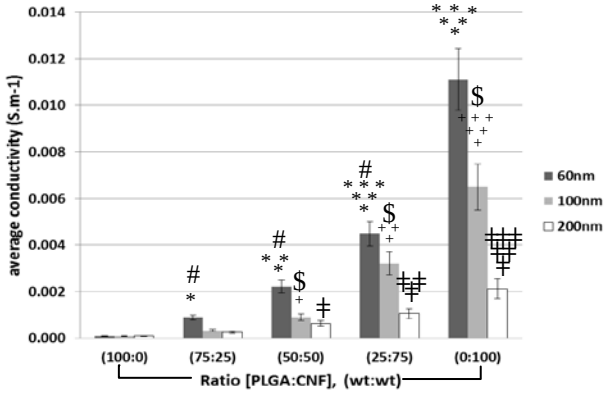

Fig**.** 1. Comparative conductivity analysis of different PLGA:CNF (wt:wt) composite ratios with different CNF diameters. Data = mean ± SEM; N =3 * $p < 0.05$ compared to the 60 nm diameter CNF 100:0 (PLGA:CNF) ratio. ** $p < 0.05$ compared to the 60 nm diameter CNF 75:25 (PLGA:CNF) ratio. *** $p < 0.05$ compared to the 60 nm diameter CNF 50:50 (PLGA:CNF) ratio. **** $p < 0.05$ compared to the 60 nm diameter CNF 25:75 (PLGA:CNF) ratio. + $p < 0.05$ compared to the 100 nm diameter CNF 100:0 (PLGA:CNF) ratio. ++ $p < 0.05$ compared to the 100 nm diameter CNF 75:25 (PLGA:CNF) ratio. +++ $p < 0.05$ compared to the 200 nm diameter CNF 50:50 (PLGA:CNF) ratio. ++++ $p < 0.05$ compared to the 100 nm diameter CNF 25:75 (PLGA:CNF) ratio. ‡ $p < 0.05$ compared to the 200 nm diameter CNF 100:0 (PLGA:CNF) ratio. ‡‡ $p < 0.05$ compared to the 200 nm diameter CNF 75:25 (PLGA:CNF) ratio. ‡‡‡ $p < 0.05$

compared to the 200 nm diameter CNF 50:50 (PLGA:CNF) ratio. ‡‡‡‡ $p < 0.05$ compared to the 200 nm diameter CNF 25:75 (PLGA:CNF) ratio.

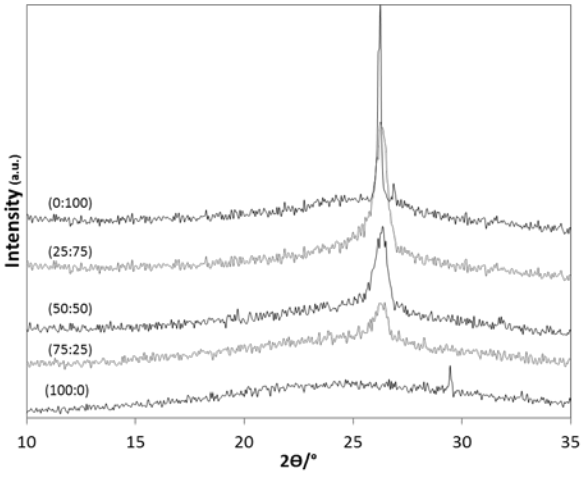

Fig. 2. XRD analysis of the 200 nm diameter PLGA:CNF composites. Measurements were completed between 10-35 degrees at a speed of 0.5 degrees per 2 minutes. Increasing the CNF weight ratio, increased the intensity and slenderness of the peak. This is due to more crystallinity of the composites, therefore the 0:100 ratio [PLGA:CNF (wt:wt)] had the most slender and intense peak.

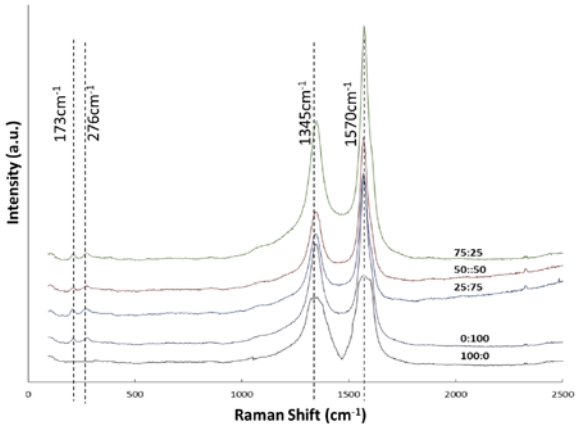

Fig. 3. Raman spectroscopy results obtained for the 200 nm CNF diameter composites of different PLGA:CNF ratios. The main peaks of consideration are 1345 and 1570 cm-1. This is due to the C-C bonds in CNFs and also in PLGA. As one decreases the PLGA PLGA concentration the amount of "different" C-C bonding decreased and the 1345 and 1570 cm^{-1} peak decreased in intensity (this is due to the addition of CNF and PLGA peaks at the same Raman shift. Peaks at 173 and 276 cm^{-1} were due to the carbon in CNFs. Similar results were found for the 100 nm diameter CNFs

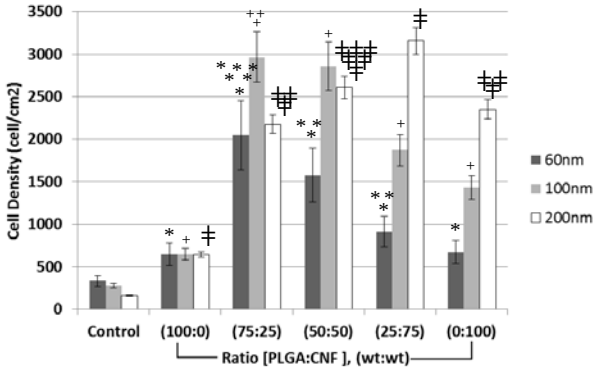

Fig. 4. Comparative cell adhesion assay of different PLGA:CNF (wt:wt) composite ratios with different CNF diameters. Data = mean ± SEM; N =3.

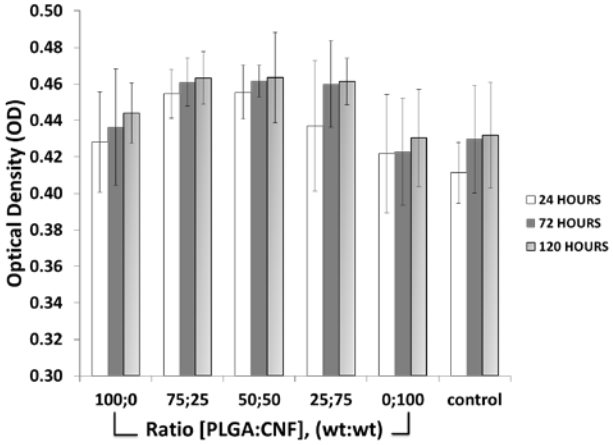

Fig. 5. Comparative Troponin-I cell proliferation assay of different PLGA:CNF (wt:wt) composite ratios on 100nm CNF diameters. Data = mean ± SEM; N =3.

8 References

[1] EF. Hirsch, M. Jellinik , T. Cooper, G. Kaiser, HC. Barner, AM. Borghard-Erdle, editors. *The innervation of the vertebrate heart*. Springfield, IL: Charles C. Thomas, 1970.

[2] L. Guth "Regeneration in the Mammalian Peripheral Nervous System". *Physiological Reviews* 1956;36: pp 441-478.

[3] M Radisic, MV Sefton. *Cardiac tissue. Principles of Regenerative Medicine* (Second edition)San Diego: Academic Press, 2011. pp 877-909.

[4] D Locca, C Bucciarelli-Ducci, G Ferrante, A La Manna, NG Keenan, A Grasso, P Barlis, F Del Furia, SK Prasad,

JC Kaski, DJ Pennell, C Di Mario. “New Universal Definition of Myocardial Infarction: Applicable After Complex Percutaneous Coronary Interventions?”. *JACC: Cardiovascular Interventions* 2010;3: pp 950-958.

[5] K Thygesen, JS Alpert, HD White. “Universal Definition of Myocardial Infarction”. *Journal of the American College of Cardiology* 2007;50: pp 2173-2195.

[6] M Barber, T Mueller, B Davies, R Gill, D Zipes. “Interruption of sympathetic and vagal-mediated afferent responses by transmural myocardial infarction”. *Circulation* 1985;72: pp 623-631.

[7] WC Randall, MP Kaye, GR Hageman, HK Jacobs, DE Euler, W Wehrmacher. “Cardiac dysrhythmias in the conscious dog after surgically induced autonomic imbalance”. *Am J Cardiol* 1976;38: pp 178-183.

[8] WRITING GROUP MEMBERS, Lloyd-Jones D, Adams R, Carnethon M, De Simone G, Ferguson TB, Flegal K, Ford E, Furie K, Go A, Greenlund K, Haase N, Hailpern S, Ho M, Howard V, Kissela B, Kittner S, Lackland D, Lisabeth L, Marelli A, McDermott M, Meigs J, Mozaffarian D, Nichol G, O'Donnell C, Roger V, Rosamond W, Sacco R, Sorlie P, Stafford R, Steinberger J, Thom T, Wasserthiel-Smoller S, Wong N, Wylie-Rosett J, Hong Y, Committee,for the American Heart Association Statistics, Stroke Statistics Subcommittee. Heart Disease and Stroke Statistics--2009 Update: A Report From the American Heart Association Statistics Committee and Stroke Statistics Subcommittee. 2009;119: pp 21-181.

[9] L Bengtsson, K Radegran, A Haegerstrand. “In vitro endothelialization of commercially available heart valve bioprostheses with cultured adult human cells”. *European Journal of Cardio-Thoracic Surgery* 1993;7: pp 393-398.

[10] CR Horres, JF Aiton, M Lieberman, EA Johnson. “Electrogenic transport in tissue cultured heart cells”. *Journal of Molecular and Cellular Cardiology* 1979;11:1201-1202, IN31, pp 1203-1205.

[11] S Ramaswamy, D Gottlieb, GC Engelmayr Jr, E Aikawa, DE Schmidt, DM Gaitan-Leon, VL Sales, JE Mayer Jr, MS Sacks. “The role of organ level conditioning on the promotion of engineered heart valve tissue development in-vitro using mesenchymal stem cells”. *Biomaterials* 2010;31: pp 1114-1125.

[12] D Schmidt, A Mol, S Neuenschwander, C Breymann, M GÃssi, G Zund, M Turina, SP Hoerstrup. “Living patches engineered from human umbilical cord derived fibroblasts and endothelial progenitor cells”. *European Journal of Cardio-Thoracic Surgery* 2005;27: pp 795-800.

[13] H Wei, C Chen, W Lee, I Chiu, S Hwang, W Lin, C Huang, Y Yeh, Y Chang, H Sung. “Bioengineered cardiac patch constructed from multilayered mesenchymal stem cells for myocardial repair”. *Biomaterials* 2008;29: pp 3547-3556.

[14] K Zitta, B Brandt, A Wuensch, P Meybohm, B Bein, M Steinfath, J Scholz, M Albrecht. “Interleukin-1[beta] regulates cell proliferation and activity of extracellular matrix remodelling enzymes in cultured primary pig heart cells”. *Biochemical and Biophysical Research Communications* 2010;399: pp 542-547.

[15] N Borenstein, V Chetboul, P Bruneval, M Hekmati, R Tissier, L Behr, G Derumeaux, D Montarras. “Non-cultured cell transplantation in an ovine model of non-ischemic heart failure”. *European Journal of Cardio-Thoracic Surgery* 2007;31: pp 444-451.

[16] J Hu, X Sun, H Ma, C Xie, YE Chen, PX Ma. “Porous nanofibrous PLLA scaffolds for vascular tissue engineering”. *Biomaterials* 2010;31: pp 7971-7977.

[17] KL Christman, AJ Vardanian, Q Fang, RE Sievers, HH Fok, RJ Lee. “Injectable Fibrin Scaffold Improves Cell Transplant Survival, Reduces Infarct Expansion, and Induces Neovasculature Formation in Ischemic Myocardium”. *Journal of the American College of Cardiology* 2004;44: pp 654-660.

[18] L Yang, BW Sheldon, TJ Webster. “The impact of diamond nanocrystallinity on osteoblast functions”. *Biomaterials* 2009;30: pp 3458-3465.

[19] S Bal. “Experimental study of mechanical and electrical properties of carbon nanofiber/epoxy composites”. *Materials & Design* 2010;31: pp 2406-2413.

[20] N Borenstein, V Chetboul, P Bruneval, M Hekmati, R Tissier, L Behr, G Derumeaux, D Montarras. “Non-cultured cell transplantation in an ovine model of non-ischemic heart failure”. *European Journal of Cardio-Thoracic Surgery* 2007;31: pp 444-451.

[21] TJ Webster, C Ergun, RH Doremus, RW Siegel, R Bizios. “Specific proteins mediate enhanced osteoblast adhesion on nanophase ceramics”. *Journal of Biomedical Materials Research* 2000;51: pp 475-483.

[22] PA Tran, L Zhang, TJ Webster. “Carbon nanofibers and carbon nanotubes in regenerative medicine”. *Advanced Drug Delivery Reviews* 2009;61: pp 1097-1114.

[23] SS Mihardja, RE Sievers, RJ Lee. “The effect of polypyrrole on arteriogenesis in an acute rat infarct model”. *Biomaterials* 2008;29: pp 4205-4210.

[24] DM Pedrotty, J Koh, BH Davis, DA Taylor, P Wolf, LE Niklason. “Engineering skeletal myoblasts: roles of three-dimensional culture and electrical stimulation”. *Am J Physiol Heart Circ Physiol* 2005;288: pp 1620-1626.

[25] KC Roberts-Thomson, PM Kistler, P Sanders, JB Morton, HM Haqqani, I Stevenson, JK Vohra, PB Sparks, JM Kalman. “Fractionated atrial electrograms during sinus rhythm: Relationship to age, voltage, and conduction velocity”. *Heart Rhythm* 2009;6: pp 587-591.

[26] L Zhang, TJ Webster. “Nanotechnology and nanomaterials: Promises for improved tissue regeneration”. *Nano Today* 2009;4: pp 66-80.